

SHEAR STRESS AND SPALL STRENGTH OF MATERIALS
UNDER SHOCK LOADS (REVIEW)

S. A. Novikov

UDC 620.171.3

Investigations of the mechanical properties of materials under shock compression are needed to predict the operability of many modern structures and for the development of new engineering treatment methods. The magnitude of the critical shear stresses on a shock front determines the condition for passage from the elastic into the plastic state. The use of piezoresistive pressure transducers permits direct measurement of the normal and tangential stresses on the wave front, whose difference characterizes the magnitude of the shear stress. Measurements performed in lead, several steels, aluminum alloys, and copper showed a practically linear increase in the shear stress with the rise in pressure on the wave front (pressure range from 10 to 130 kbar). The strongest dependence is detected in lead. The results obtained indicate a more complex pattern of the phenomenon than that which follows from elastic-plastic theory taking account of the influence of hydrostatic pressure on the magnitude of the shear stress.

The energy criterion, representing the equality of the elastic and the rupture energies, is one of the most widespread for the description of the spall phenomenon. The minimal effective value of the rupture energy γ_{\min} can be estimated from test results on the loading of specimens by a grazing detonation wave. Values of γ_{\min} for 13 metals and three plastics, obtained under identical loading conditions, are represented.

Results of investigating the dependence of the spall strength of a whole series of metals and alloys on the temperature in the range 196–800°C showed that the spall process is not athermal. Investigation of the microstructure of specimens subjected to shock loading permits relating the temperature dependence of the spall strength to a different rupture mechanism in a broad temperature test range.

1. INVESTIGATIONS OF THE SHEAR STRESS

The stress state of a volume element under shock compression in uniaxial strain conditions is characterized by two principal stresses, P_n the stress acting on an area perpendicular to the wave propagation direction, and P_τ the stress acting on areas parallel to the direction of its propagation. The maximum tangential (shear) stresses τ in a homogeneous substance act on planes located at a 45° angle to the plane of the shock front $2\tau = P_n - P_\tau$. The mean (hydrostatic) pressure in a volume element is $P = (P_n + 2P_\tau)/3$, from which $P_n = P + (4/3)\tau$. This relationship determines the mutual location of the shock adiabat and the hydrostatic compression curve.

It is assumed in the simplest theories of elasticity and plasticity that the magnitude of the shear stresses remains constant upon loading a material above the elastic limit. In the Coulomb-Navier theory of tangential stresses, a dependence of the critical shear stresses on the magnitude of the normal pressure on an area is introduced by using the internal friction coefficient ν

$$|\tau| = \tau_0 - \nu P$$

(τ_0 is the shear stress for $P = 0$, the negative sign in the formula corresponds to positive P under tension). Measurements of the shear strength under high static pressures in the known researches of P. Bridgman and L. F. Vereshchagin displayed their significant increase as the pressure rose. A strong dependence of the critical shear stresses on the magnitude of the pressure in the shock front was detected also in the first experiments on shock compression of metals [1-4].

TABLE 1

| Material under investigation | Stress | | Magnitude of the shear stress 2τ , kbar |
|------------------------------|---------------------|--------------------------|---|
| | normal P_n , kbar | tangential, P_t , kbar | |
| St. 3 | 12,0 | 5,0 | 7,0 |
| » | 46,5 | 31,0 | 15,5 |
| » | 52,0 | 35,0 | 17,0 |
| » | 62,0 | 41,0 | 21,0 |
| » | 66,0 | 44,0 | 22,0 |
| » | 83,0 | 57,0 | 26,0 |
| » | 102,0 | 72,0 | 30,0 |
| » | 130,0 | 93,0 | 37,0 |
| St. 45 | 70,0 | 44,0 | 26,0 |
| » | 71,0 | 44,0 | 27,0 |
| » | 130,0 | 93,0 | 37,0 |
| AMg-6 aluminum | 20,5 | 18,5 | 2,0 |
| » | 42,0 | 39,0 | 3,0 |
| » | 49,0 | 45,0 | 4,0 |
| » | 75,0 | 69,0 | 6,0 |
| AD-1 aluminum | 37,0 | 32,0 | 5,0 |
| » | 78,0 | 55,0 | 23,0 |
| » | 119,0 | 91,0 | 28,0 |
| S-4 lead | 23,0 | 10,0 | 13,0 |
| » | 45,0 | 21,0 | 24,0 |
| » | 46,0 | 17,0 | 29,0 |
| » | 56,0 | 23,0 | 33,0 |
| » | 58,0 | 22,0 | 36,0 |
| » | 59,0 | 26,0 | 33,0 |
| » | 77,0 | 27,0 | 50,0 |
| » | 95,0 | 40,0 | 55,0 |
| M1 copper | 24,0 | 19,5 | 4,5 |
| » | 62,0 | 52,0 | 10,0 |
| » | 68,0 | 60,0 | 8,0 |
| » | 111,0 | 94,0 | 17,0 |

Until recently, an indirect method of "overtaking unloading," based on a study of the attenuation of a shock excited in a material by the impact of plate, was used to determine the magnitudes of the critical shear stresses behind a shock front. The magnitudes of the critical shear stresses were estimated from a comparison between the experimental dependences of shock attenuation in the specimen [1-5] and a series of computed dependences obtained for different amplitudes of the elastic unloading wave. That value at which the best agreement with experiment was obtained was taken as the desired quantity. The magnitude of the critical shear stress in copper (3.5 kbar) was estimated by computational means in [6] from the results of experiments in which the radius of the cavity being formed upon unloading continuous spheres after they had been compressed by a spherically-symmetric shock was determined. The possibility of measuring the shear stress under shock compression as the difference between two principal stresses at the shock front appeared with the development of methods of measuring pulse pressures by using manganin and dielectric transducers. In these experiments, transducers of quite small thickness were inserted into slits made in the material perpendicularly and in parallel to the shock front being propagated therein. Because of the small transducer dimensions, their influence on the pattern of the wave processes in the material is negligible. Magnitudes of the principal stresses P_n and P_t are measured directly in tests. To produce shock pressures of different magnitude in the materials under investigation, explosive loading units of the "flake" type were used in [7] (see [8], for example). The loading was realized through a shield of steel, copper, aluminum, Plexiglas, polyethylene. The pressure transducers were fabricated from 0.05 mm diameter manganin wire with copper foil leads 0.04 mm thick and 2 mm wide. The transducer insulation was from fluoroplastic, Lavsan, or mica films. The total transducer thickness was 0.20-0.25 mm, the resistance was 3-5 Ω , and the magnitude of the working current was approximately 10 A. The recording was by a bridge circuit using an OK-33 oscilloscope. The sensitivity of the measuring channel was not less than 0.04 V/kbar, and the error in the pressure measurement did not exceed 10%.

The results of the investigations performed are represented in Table 1 and in Fig. 1 in the coordinates 2τ , P_n . Some data of other authors are presented there: the results of analogous investigations using manganin and dielectric transducers [9-11] (1 - lead [7]; 2 - St-3 [7]; 3 - St. 45 [7]; 4 - St. 20 [10, 11]; 5 - St. 20 [7]; 6 - copper [7]; 7 - AD-1 aluminum [7]; 8 - AMg-6 aluminum [7]; 9 - V95 aluminum [11]), as well as results of measuring

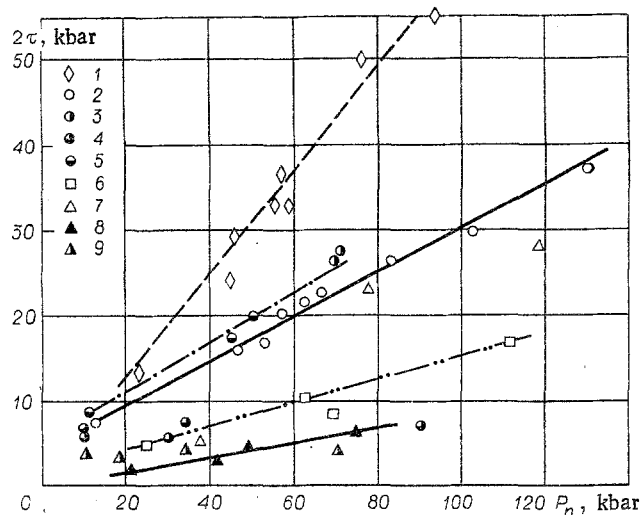


Fig. 1

the Hugoniot pressure in elastic compression waves [12-14]. These latter are of interest for relatively moderate shock compression pressures.

The magnitude of the Hugoniot elastic limit (P_H), determined by the breakpoint on the shock compression adiabat for the material, and sometimes called the dynamic yield point, is related to the yield point under simple compression ($\sigma_d = 2\tau$) by the relationship

$$P_H = \frac{1 - \mu}{1 - 2\mu} \sigma_d.$$

The dependences represented in Fig. 1 characterize a practically linear increase in the magnitude of the critical shear stresses behind the shock front due to the pressure. The maximal magnitude of the pressure in the shock in the results presented is obtained in steel specimens and is 130 kbar, i.e., equals the pressure of the phase transition ($\alpha \rightarrow \epsilon$) in iron under shock compression. In this connection, it should be noted that for the two steels investigated in this paper (St. 3 and St. 45), the magnitudes of the shear stresses near the phase transition point are in agreement while they differ noticeably in the intermediate domain (from the Hugoniot pressure to the phase transition pressure). The magnitude of the shear stress for St. 3 and St. 45 near the phase transition point is just one-third the theoretical strength for steel ($\tau_T = G/15$, G is the shear modulus). That the hydrostatic pressure curve for St. 3 [7], computed by means of the measured values of P_n and P_τ , is in good agreement with the known hydrostatic compression curve for this steel can be confirmation of confidence in the results obtained under shock loading.

The results of measuring τ in shock experiments for St. 45 [7] lie noticeably above the static investigation data [15]. The same discrepancy holds also for certain other metals. Let us note that the stress state under static conditions is inhomogeneous over the specimen section, consequently τ should be a certain average characteristic of the shear strength. Performing a detailed analysis of static experiments to compare with shocks is quite a complex problem. In this connection, it should be emphasized that the specimen material in [7] (loading by a stationary wave of definite duration by using "flakes") was practically under constant conditions for $\sim 2 \mu\text{sec}$ behind the shock front. Hence, to explain the discrepancy between the data and the static results because the loading is "dynamic" would seem to assume that the relaxation time of the tangential stresses is quite large ($\geq 2 \mu\text{sec}$), which is apparently of low probability. The data in [10, 11] for St. 20 contradict the results presented and the data of static investigations. An increase in the shear strength of St. 20 to a 90 kbar pressure is not recorded in the papers mentioned. An increase in the shear strength for the aluminum alloy V95 at a 70 kbar pressure is also not detected in [10]. This diverges from the general physical representations about the influence of pressure on the magnitude of the shear stress. It is possible that the reason is methodological errors associated with the use of a dielectric transducer in these papers, whose operating mechanism had not been investigated completely yet. Thus, for example, it was shown in the experiments we performed using dielectric Lavsans, fluoroplastic, and mica transducers that under the effect of two successive compression waves on a transducer, it stably (severalfold) reduces

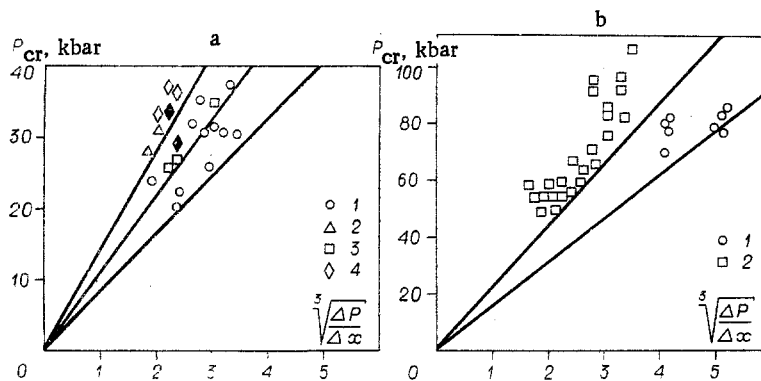


Fig. 2

the amplitude of the second wave while completely reproducing the time nature of the shock profile record obtained by using a manganin pressure transducer and a capacitive velocity transducer. The results of the investigations performed showed that this reduction can be explained only by an abrupt change in the physical properties of the dielectrics under repeated shock compressions. Therefore, the method of measuring pulse pressures by the dielectric transducer method does not permit the recording of a multiwave shock configuration. It can consequently be assumed that initially an elastic predecessor acted on the transducer in the tests described in [10], and then a second wave, whose pressure could be reduced in conformity with the phenomenon noted. For the two aluminum alloys investigated (AD-1 and AMg-6), the dependence of the resistance to shear lies above for the alloy AD-1. A similar phenomenon is detected in [16] in investigations of the dynamic tension diagrams of these alloys.

The unexpectedly strong dependence of the shear stress on the pressure in a shock is obtained for lead. If it is taken into account that the shear stress behind a shock front is practically zero for a 400 kbar pressure in the shock in [3], as is confirmed by the fact of lead melting under these shock compression conditions, then it should be considered that a sufficiently abrupt rise in the shear stress occurs in lead in the pressure range from zero to 400 kbar, with a subsequent diminution to zero.

The results of experimental investigations represented, particularly the stronger dependence of the shear stress under shock loading than in static experiments, the unexpectedly significant rise in the shear stress for lead, the difference in the behavior of aluminum alloys, indicate a more complex pattern of the phenomenon than that which follows from elastic-plastic theory, of taking account of the influence of the hydrostatic pressure on the magnitude of the shear stress. For a detailed analysis of the influence of the shear stress on the shock compression of materials, it is necessary to rely on a more complex model, for instance, a viscoelastic plastic body, as a number of authors has already noted (see [17], say).

2. INVESTIGATION OF THE RUPTURE STRESSES UNDER SPALLING

The tensile stresses in a material subjected to shock loading that result in spall rupture occur during the interaction between rarefaction waves reflected from free surfaces and propagated behind a compression wave front. In computational-experimental methods of investigating the spall phenomenon, the resistance of the material to shear stresses is often neglected (hydrodynamic approximation). The change in entropy can also be neglected in an examination of not too strong shocks (quasiacoustic approximation) by considering that the pressure is a function of just the density, while the shock adiabat and the expansion isentrope coincide. It is impossible to neglect the change in entropy under the action of strong shocks while the influence of the shear stress is insignificant. In this case, the equation of state is used in the Mie-Grüneisen form. Experimental investigations of the spall phenomenon, performed in the 50's and 60's, showed that the spall strength is not a constant characteristic for a given material, but depends to a strong degree on the conditions of conducting the test. The deduction that the rupture criterion during spall should include the time interval during which tensile stresses exist in the material was first made in [18]. The process of rupture during spall consists of the generation of microcracks in the weakest areas of the material, and their development and merger into mainline crack separating the material, i.e., it requires a definite time interval dependent on the prehistory of the stress state (from the earliest papers, see [19-22], for instance). Recently, the kinetic theory of the rup-

TABLE 2

| Material | h_1 , mm | h_2 , mm | γ_{\min} j/cm ² |
|---|------------|------------|--------------------------------------|
| AD-1 aluminum [26] Aluminum alloy D16 (quenched) [26] | 0,3-2,6 | 2-12 | 1,25 |
| Aluminum alloy D16 (annealed) [26] | 0,5-1,8 | 10 | 7,10 |
| Aluminum alloy AMts [28] | 0,4-1,1 | 10 | 2,65 |
| Aluminum alloy AMg [29] | 0,5-2,2 | 2-15 | 1,21 |
| M1 copper [26] | 3-5 | 8 | 6,53 |
| NP2 nickel [2] | 0,3-1,5 | 2-12 | 0,60 |
| PS1 lead [26] | 0,3-1,6 | 2-4 | 2,97 |
| St. 3 [30, 29] | 0,3-0,5 | 8-12 | 0,11 |
| St. 3 [26] | 3-5 | 5-40 | 9,15 |
| S418-36 cast iron [26] | 0,3-1,6 | 2-4 | 3,30 |
| 12Kh18N10T steel [26] | 0,5-0,8 | 4 | 0,43 |
| VT3 and VT14 titanium [26] | 0,8-2,6 | 2-4 | 35 |
| Polytetrafluoroethylene | 0,8-2,6 | 2-4 | 47 |
| Plexiglas [26] | 0,3-0,1 | 3-15 | 0,28 |
| Polyethylene [26] | 0,3-0,9 | 10-20 | 0,15 |
| | 0,3-0,6 | 5-20 | 0,05 |

ture of solids, relating the longevity of the solid to the magnitude of the stress and the temperature and confirmed by extensive experimental material in the domain of a 10^{-3} sec and higher load action time, has received extensive propagation. The inapplicability of the kinetic theory in the range of short times (10^{-6} sec and less) has been noted repeatedly, i.e., in the description of spall phenomena. A detailed survey of existing rupture criteria during spall is presented in [23]. One is the energetic spalling criterion representing the equality of the elastic energy in the tension pulse to the work performed in separating the material (the rupture energy) γ . The mean energy needed to separate a material can be estimated by knowing the characteristic time of operation of the negative stress P_{CR} causing the spalling rupture. The kinetics of the development and merger of the cracks in the rupture domain is not considered here. Let us note that the total area of the surface being formed during spall (i.e., during interaction of the cracks) should depend on the nature of crack propagation (on their velocity, see [24]). Nevertheless, the quantity γ defined in conformity with this criterion for different materials in tests of identical formulation should apparently yield a sufficiently objective comparative pattern of material behavior under spall. Experimental data on the rupture energy of different steels are presented in [25].

Among the simple computational-experimental methods of investigating the spall phenomenon is the case of loading by using a grazing detonation wave in a thin layer of explosive material (HE).

The use of plastic HE makes this the simplest method in technical respects. A plastic HE with a 1.52 g/cm^3 density and 7.8 km/sec detonation rate was used in [26]. The HE strip superposed on the surface of the specimen being investigated was initiated by using a linear detonation wave generator from a perforated plastic HE. The nature of the spall rupture was observed visually after the loading, and the thickness of the spall layer was measured. A numerical computation of the flow field in the explosion products (EP) and the loaded material was performed by the method of characteristics. The method of computation is described in detail in [27]. The expansion isentrope of the EP was taken in the form of a cubic polytrope, and the equations of state of the materials were taken without taking account of the strength and the change in entropy, in the form of known linear relationships between the wave and mass flow velocities. The maximal negative pressure in the rupture plane and the pressure gradient $\Delta P/\Delta x$ in the tensile pulse, whose shape is almost triangular in this case, were determined in the computations.

To estimate the correctness of the computations, the parameters of the shock emerging on the free surface (the pressure in the wave front, the free surface velocity) were measured, which exhibited completely satisfactory agreement between the computed and experimental data

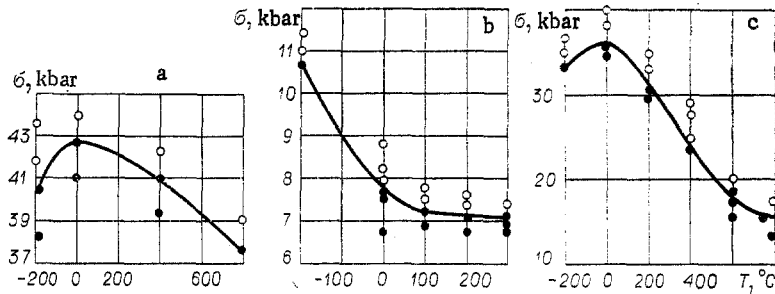


Fig. 3

for plastic metals and polymers.* Some results of processing the data obtained are represented in Fig. 2 in the coordinates $P_{cr} \sqrt[3]{\frac{\Delta P}{\Delta x}}$ (a, the point 1 is the aluminum alloy AMts [28], 2 is the aluminum alloy AMg [29], 3 is the alloy D16 (annealed) [26], 4 is the alloy D16 (quenched) [26]; b, the point 1 is St. 3 [26], 2 is St. 3 [30, 29]). Such a selection of coordinates is due to the attempt to systematize the experiment results from the viewpoint of the above-mentioned energetic spalling rupture criterion. In application to the results of this paper, this criterion can be represented in the form

$$P_{cr}^3 \left(\frac{\Delta P}{\Delta x} \right) = 6 \rho_0 c_0^2 \gamma \quad (2.1)$$

(ρ_0 is the density, and c_0 is the volume speed of sound). In the mentioned coordinates, the results of tests in which the presence of absence of spall in this material was determined can be delimited by a line from the origin and separating the spalling rupture zone, and conserving the continuity of the material. As follows from (2.1), the slope of this line determines the magnitude of the minimal rupture energy γ_{min} . The rupture energy values obtained in this manner are represented in Table 2. The ranges of variation of the HE layer thickness h_1 and specimen thickness h_2 are given there. It can be asserted that spalling rupture will not occur under analogous or almost similar conditions of shock loading if the elastic energy in the tension pulse does not exceed the value γ_{min} obtained in this manner. Comparing the values of γ_{min} obtained with the results of other authors [31-34], obtained in tests with explosive loading by an HE charge from a plane detonation wave or under impact by a plate, displays a noticeable increase in the values of the rupture energy in the latter papers. This can be explained not only by the fact that the data represented in Table 2 characterize the minimal rupture energy, but principally also by the influence of the system scale. This is indicated, for instance, by the increase in γ to 9 J/cm² for St. 3 [30] under analogous loading (grazing detonation) and an increase in the scale and a diminution in γ for aluminum 6061-T6 to 1 J/cm² [35] under loading by the impact of a plate and a diminution in the system scale. This is apparently related to the fact that crack origination occurs in a volume whose size is commensurate with the size of the loading pulse, i.e., the energy going into rupture is proportional in a first approximation to the system scale.

Investigations of the spalling strength at elevated temperatures when the dependence of the magnitude of the rupturing stresses P_{cr} on the time should appear more clearly are of considerable practical and scientific interest. A comparatively weak diminution in the P_{cr} of steel and copper was detected in the first papers devoted to this question [36, 37], as the specimen temperature rose. On the basis of the results of tests they performed, the authors of [38] made the deduction that the process of metal rupture is almost athermal for longevities in the microsecond range. Values of the spalling strength of aluminum alloy AMg-6 were first obtained in [39] for a broad range of temperatures up to the melting point (around 600°). A sufficiently rapid diminution in the spalling strength was detected with the rise in temperature above 200°C. The rupture energy at $T = 500^\circ\text{C}$ turned out to be one-sixth that at normal temperature (the loading was accomplished by the impact of a plate). The results of further investigations, part of which is elucidated in [31], also do not agree with the deduction [38] about athermy of the spalling rupture of metals. Specimens from St. 3, 12Kh18N10T steel, M1 copper, AD-1 aluminum, the aluminum alloy D16, S2 lead, and VT-14

*In the case of loading metals possessing considerable shear strength, shock attenuation will be more intense, and the computation yields only the upper bound for the shock amplitude.

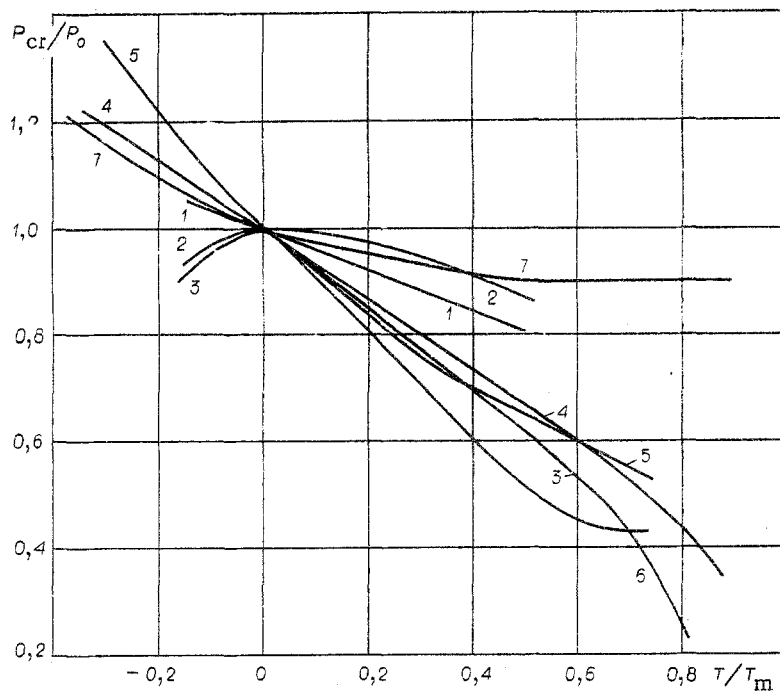


Fig. 4

titanium were investigated in [31] in a broad temperature band. The specimens of the metals under investigation were fabricated from material in the factory delivery state. The loading was by the impact of an aluminum plate accelerated to a given velocity by the grazing detonation of a plastic HE. Specimen heating was by the radiant heat flux from a heater. The specimens were cooled to the temperature -196°C by submersion in a vessel with liquid nitrogen. Specimens of the material under investigation were brought to total separation (to the formation of a mainline crack) in a series of tests with a successive stepwise increase in the velocity of the impactor plate. The magnitude of the tensile stresses in the spall plane was determined by a computational method. The validity of the computations was confirmed by the results of direct pressure measurements. The loading time was $1.3 \mu\text{sec}$. Some of the dependences $P_{\text{cr}} = f(T)$ constructed in this manner are presented in Fig. 3 (a, St. 3; b, S2 lead; c, M1 copper). Curves are drawn through the experimental points corresponding to the formation of a mainline crack (— mainline \circ crack present; \bullet — crack absent). Dependences of the spall strength on the temperature are constructed in Fig. 4 in the dimensionless coordinates (P_{cr}/P_0 , T/T_m) for the metals investigated (T_m is the melting point, P_0 is the spall strength determined in these experiments at 0°C , which is 17.5 kbar for AD-1, 23.2 kbar for D16; 24.4 kbar for AMg-6; 38.9 kbar for St. 3; 54 kbar for the steel 12Kh18N10T; 48.1 kbar for VT-14 titanium; and 34.3 kbar M1 for copper). Line 1 is VT-14 titanium, 2 is St. 3, 3 is M1 copper, 4 is AD-1 aluminum, 5 is the aluminum alloy D16, 6 is the aluminum alloy AMg-6, and 7 is S2 lead. The graph demonstrates the noticeable difference in metal behavior in the considered temperature range. The diminution in the spall strength of steel and copper at negative temperatures as well as the fact that the magnitude of the spall strength of metals is a significant quantity as the melting point is approached, should be noted. The experimental results obtained indicate that the temperature substantially affects the crack origination and development during spall. A temperature rise results in a certain activation of the dislocation mechanisms of crack origination, which results in a reduction in the critical level of the rupturing stresses. Lowering the temperature results also in a change in the rupture characteristic from viscous to brittle, which also specifies a reduction in the rupture stress level for some metals at the temperature -196°C .

A study of the microstructure of specimens in the domain of rarefaction wave interaction that results in rupture yields valuable information about the spalling rupture mechanism for metals at different temperatures. For example, intense twinning in the ferrite grains is observed in St. 3 at the temperature -196°C in practically the whole bulk of specimen, while twinning occurs at the temperatures 0°C and 400°C only near the impact surface. Microcrack origination in St. 3 occurs over the whole bulk at -196°C (in the ferrite and perlite

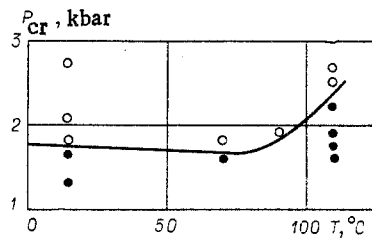


Fig. 5

grains, on the grain boundaries, in inclusions). At 0°C microcracks originate mainly on the ferrite grain boundaries. Microcrack origination starts at 400°C and 800°C at the sulfide inclusions in the ferrite. The development of spalling rupture and the formation of a main-line crack occur because of pore growth and cracking of the material between the pores. The reduction in the spall strength of St. 3 at negative temperatures (Fig. 3a) is related to the increase in the quantity of centers of microcrack origination and the more brittle nature of their development. A comparatively small diminution in the spall strength during heating is related to the diminution in the number of crack origination centers. The noticeable hardening during cooling for 12Kh18N10T steel (Fig. 4) is caused by the phase transition of austenite into martensite that occurs under shock compression at these temperatures. A considerably stronger diminution in the spall strength occurs during heating of 12Kh18N10T steel specimens as compared with St. 3, which can be related to the increase in the number of inclusions separated out from the solid solution during heating. Investigations of the microstructure of a whole series of metals showed that the individual nature of the temperature dependence of the spall strength for each can be explained by a different mechanism for the origination and propagation of cracks in a broad temperature range. It is hence impossible to speak about the athermy of the rupture process in the "microsecond" loading range on the basis of just the weak temperature dependence of the crack propagation velocity (the speed of sound).

Experiments we performed with Plexiglas in the temperature range from 0°C to 110°C demonstrate the noticeable dependence of the spall strength on the nature of rupture development. Loading was by the impact of an aluminum plate, analogously to [31], and the characteristic loading time was 1.5 μsec. The dependence obtained is represented in Fig. 5. The spall strength of Plexiglas near the temperature 110°C (softening temperature) grows by approximately 30% as compared to 0°C. It can be assumed that the passage of Plexiglas into the softened state at T = 110°C results in a significant change in the nature of the spall rupture (from brittle to viscous), and therefore in an increase in the rupture viscosity and the uniquely related rupture energy.

Experimental investigations recently performed permitted a more detailed representation of material behavior under intense short-range loads. They showed that the most important mechanical properties of materials subjected to shock loading in the practically important range of pressures to several hundred kilobars cannot be described by using simple computational models. Further development in this area requires continuation of the studies in the high temperature range and "ultrashort" (to 10⁻⁸ sec) characteristic times of tensile stress action.

LITERATURE CITED

1. D. R. Curran, "Nonhydrodynamic attenuation of shock waves in aluminum," *J. Appl. Phys.*, **34**, No. 9 (1963).
2. S. A. Novikov and L. M. Sinitsyna, "On the role of strength in unloading a shock-compressed medium," in: *Summaries of Reports. II. All-Union Symposium on Combustion and Explosion [in Russian]*, Erevan (1969).
3. S. A. Novikov and L. M. Sinitsyna, "Investigation of critical shear stresses behind a shock front in metals," *Prikl. Mekh. Tekh. Fiz.*, No. 6 (1970).
4. L. V. Al'tshuler, M. I. Brazhnik, and G. S. Telegin, "Strength and elasticity of iron and copper under high shock compression pressures," *Zh. Prikl. Mekh. Tekh. Fiz.*, No. 6 (1971).
5. Yu. V. Bat'kov, S. A. Novikov, et al., "Investigation of Plexiglas and textolite expansion adiabat from the shock-compressed state at 30 kbar pressure," *Mekh. Kompozitn. Mater.*, No. 2 (1979).

6. S. M. Bakhrakh, N. P. Kovalev, S. A. Novikov, et al., "Investigation of the plastic and strength properties of copper under multilateral compression," *Dokl. Akad. Nauk SSSR*, 215, No. 5 (1974).
7. Yu. V. Bat'kov, S. A. Novikov, et al., "Investigation of shear stresses in metals on a shock front," *Zh. Prikl. Mekh. Tekh. Fiz.*, No. 6 (1980).
8. L. V. Al'tshuler, "Application of shocks in high pressure physics," *Usp. Fiz. Nauk*, 85, No. 2 (1965).
9. A. N. Dremin and G. I. Kanel', "Compression and rarefaction waves in shock-compressed metals," *Zh. Prikl. Mekh. Tekh. Fiz.*, No. 2 (1976).
10. V. A. Astanin, "Investigation of the resistance of materials to strain under the effect of plane elastic-plastic waves," Abstract of Candidate's Dissertation, IPP Akad. Nauk Ukr. SSR, Kiev (1978).
11. G. V. Stepanov and V. A. Astanin, "Determination of the resistance of a material to shear behind a plane shock front," *Probl. Prochn.*, No. 4 (1976).
12. S. A. Novikov, V. A. Sinitsyn, et al., "Elastic-plastic properties of a number of metals under explosive loading," *Fiz. Met. Metalloved.*, 23, No. 3 (1966).
13. G. R. Fowles, "Shock wave compression of hardened and annealed 2024 aluminum," *J. Appl. Phys.*, 32, No. 8 (1961).
14. High-Speed Shock Phenomena. Collection [Russian translation], Mir, Moscow (1973).
15. V. A. Shapochkin, "Mechanical properties of special steels and alloys under high hydrostatic pressure," *Fiz. Met. Metalloved.*, 9, No. 2 (1960).
16. A. P. Bol'shakov, S. A. Novikov, et al., "On obtaining the tension diagram of specimens under explosive loading," *Zh. Prikl. Mekh. Tekh. Fiz.*, No. 1 (1975).
17. G. I. Kanel', "Viscoelastic properties of metals in a shock," in: *Detonation* [in Russian], Chernogolovka (1978).
18. B. M. Bucher, L. M. Barker, et al., "Spall in metals," *AIAA J.*, 2, No. 6 (1964).
19. Yu. I. Tarasov, "Investigation of the dependence of the time to rupture on the tensile load for steel and copper," *Dokl. Akad. Nauk SSSR*, 165, No. 2 (1965).
20. L. V. Al'tshuler, S. A. Novikov, and I. I. Divnov, "Relation of the critical rupturing stresses to the time to rupture for explosive loading of metals," *Dokl. Akad. Nauk SSSR*, 166, No. 1 (1966).
21. N. A. Zlatin and B. S. Ioffe, "On the time dependence of the resistance to separation during spall," *Zh. Tekh. Fiz.*, 42, No. 8 (1972).
22. S. A. Novikov and L. M. Sinitsyna, "On the influence of the strain rate during spall on the magnitude of the rupture stress," *Fiz. Met. Metalloved.*, 28, No. 6 (1969).
23. Yu. I. Fadeenko, "Time rupture criteria in solid state dynamics," in: *Dynamical Problems of the Mechanics of a Continuous Medium* [in Russian], Institute of Hydrodynamics, Siberian Branch, Academy of Sciences of the USSR, Novosibirsk (1977).
24. A. S. Eremenko, S. A. Novikov, and A. P. Pogorelov, "Investigation of fast crack propagation and interaction in organic glass," *Zh. Prikl. Mekh. Tekh. Fiz.*, No. 4 (1979).
25. A. G. Ivanov and V. N. Mineev, "On scale effects during rupture," *Fiz. Goreniya Vzryva*, No. 5 (1979).
26. V. K. Golubev, S. A. Novikov, and L. M. Sinitsyna, "On rupture of materials under loading by the explosion of a sheet HE charge," *Zh. Prikl. Mekh. Tekh. Fiz.*, No. 2 (1981).
27. Yu. M. Privalov, V. R. Soloneko, and B. A. Tarasov, "Effect of a grazing detonation on a compressible wall," *Fiz. Goreniya Vzryva*, No. 3 (1976).
28. E. V. Menteshov, V. P. Ratnikov, et al., "Effect of the explosion of a sheet explosive charge on an aluminum plate," *Fiz. Goreniya Vzryva*, No. 2 (1967).
29. A. P. Rybakov, E. V. Menteshov, et al., "Effect of the explosion of a sheet explosive charge on metal plates," *Fiz. Goreniya Vzryva*, No. 1 (1968).
30. A. P. Rybakov, "Spall's in steel under loading by using the explosion of a sheet HE charge and impact by a plate," *Zh. Prikl. Mekh. Tekh. Fiz.*, No. 1 (1977).
31. S. A. Novikov, V. K. Golubev, et al., "Influence of temperature on the magnitude of the rupture stress during spall in metals," in: *Applied Problems of Strength and Plasticity* [in Russian], No. 11, Gor'kii State Univ. Press, Gor'kii (1979).
32. B. R. Breed, C. L. Mader, and D. Venable, "Technique for the determination of dynamic tensile-strength characteristics," *J. Appl. Phys.*, 38, No. 8 (1967).
33. G. Nahmani, "Experimental investigation of scabbing produced in mild steel plates by plane stress waves," in: *Les Ondes de Detonation*. CNRS, Paris (1962).
34. B. A. Tarasov, "On a quantitative description of spall damage," *Zh. Prikl. Mekh. Tekh. Fiz.*, No. 6 (1973).

35. L. J. Cohen and H. M. Berkowitz, "Time dependent fracture criteria for 6061-T6 aluminum under stress-wave loading in uniaxial strain," *Int. J. Fracture Mech.*, 7, No. 2 (1971).
36. S. A. Novikov, I. I. Divnov, and A. G. Ivanov, "Investigation of the rupture of steel, copper, and aluminum under explosive loading," *Fiz. Met. Metalloved.*, 21, No. 4 (1966).
37. S. A. Novikov, Yu. S. Sobolev, et al., "Investigation of the influence of the temperature on the magnitude of the rupture stress during spall in copper," *Probl. Prochn.*, No. 3 (1977).
38. N. A. Zlatin, G. S. Pugachev, et al., "Time dependence of the strength of metals for microsecond band longevities," *Fiz. Tverd. Tela*, 17, No. 9 (1975).
39. Yu. V. Bat'kov, S. A. Novikov, et al., "Influence of the specimen temperature on the magnitude of the rupture stress during spall in the aluminum alloy AMg-6," *Zh. Prikl. Mekh. Tekh. Fiz.*, No. 3 (1979).

MODELING OF SPALLING RUPTURE UNDER SHOCK DEFORMATION.

ANALYSIS OF AN INSTANTANEOUS SPALLING SCHEME

N. Kh. Akhmadeev and R. I. Nigmatulin

UDC 539.42:620.172.254

1. Spalling of the rear part of a specimen being loaded [1, 2] is observed during shock or explosive loading of metal targets when the shock being generated is of sufficient intensity and emerges on the free surface. Experimental investigations of this phenomenon in [3, 4] are devoted mainly to the determination of the time dependence of the specimen strength in the spall section for loads of duration $\sim 10^{-6}$ sec. On the basis of the data from these experiments, one of the deductions [4] is the determination of the spalling rupture process as a multifocus process, when there occur a large number of microcracks in the tensile force zone, which merge in their further development into a single large crack separating the specimen into two parts. A group of papers [1, 5-8] represents the results of experimental investigations of spalling rupture stresses under shock and explosive deformation of specimens of different materials. Analysis of these papers results in the following fundamental conclusion: For each of the materials tested there is a significant spread in the calculated (by acoustic theory) values of the spalling rupturing stresses, that vary substantially as a function of the experiment conditions. Part of the spall experiments (see [6, 9], say) is devoted to determining the threshold values of the impactor flight velocity corresponding to the origination of initial damage (or micropores, microcracks) in the tension wave, and to the formation of total spalling rupture. It should be noted that because of the great complexity and for a more unique treatment, the experiments are performed mainly in a plane formulation permitting the clarification of the most characteristic features of the phenomenon being studied. Considerable difficulties must also be encountered in a numerical modeling of the shock and explosive loading of specimens. The mathematical models proposed for the nonstationary shockwave flows are a system of nonlinear partial differential equations, and they can be investigated completely only by using powerful computers.

Especially necessary in a numerical investigation of the propagation of an initiated shock pulse is taking correct account of the different physicochemical processes occurring in the shocks and the rarefaction waves — for instance, taking account of the elastic-plastic and phase transitions resulting in the formation of a multiwave profile of the shock pulse, taking account of wave interaction on the contact and free boundaries, etc. The shock loading method and the history of flow development can alter the whole wave pattern to a significant extent. Hence, constant correlation of the results of a computation with the data of full-scale tests is necessary. An elastic-plastic model of a two-phase continuous medium with physicochemical transformations is developed in [10, 11], that permits modeling processes occurring during the high-speed collision of two plates of length l_1 and l_2 and complicated by phase transformations. Modeling the motion of detonation waves and the loading process of iron and nickel specimens by the explosion of a superposed high-explosive charge of crystalline and porous hexogen is executed in [12, 13]. On the basis of the elastic-plastic model proposed in [10, 11], a numerical investigation is performed in this paper for the process